J. Synchrotron Rad. (1998). **5**, 741–743

A new compact spin- and angle-resolving photoelectron spectrometer with a high efficiency

S. Qiao,[a,b]* A. Kimura,[a] A. Harasawa[a] and A. Kakizaki[a]

[a]*Synchrotron Radiation Laboratory, Institute for Solid State Physics, University of Tokyo, Minato-ku, Tokyo 106, Japan, and* [b]*Surface and Interface Engineering Laboratory, The Institute of Physical and Chemical Research (RIKEN), Hirosawa 2-1, Wako, Saitama 351-01, Japan. E-mail: qiao@postman.riken.go.jp*

(*Received 4 August 1997; accepted 8 December 1997*)

A portable spin- and angle-resolving photoelectron spectrometer has been constructed, equipped with a newly developed compact retarding-potential Mott-scattering electron spin polarimeter with an efficiency of 1.9×10^{-4} for a gold target. Based on Monte Carlo calculations for the spin-dependent electron-scattering process and electron ray-tracing calculations, a novel design of the retarding-field electron optics with 0.59 sr collection solid angle for scattered electrons has been accomplished. Utilizing this spectrometer, the spin- and angle-resolved photoelectron spectra have been measured and the spin-dependent electronic structure of Ni(110), Ni(110)-$p(2 \times 1)$O and Ni(110)-$c(2 \times 2)$S along the $\overline{\Gamma S}$ line of the Ni(110) surface Brillouin zone have been studied.

Keywords: spin- and angle-resolved photoelectron spectroscopy; Mott polarimeters.

1. Introduction

Spin- and angle-resolved photoelectron spectroscopy (SARPES) has been increasing in importance as one of the feasible experimental techniques to investigate directly the spin-dependent electronic structures of magnetic and non-magnetic materials (Feder, 1985). Among many spin-dependent electron-scattering processes that are utilized to accomplish the electron spin polarization measurements, Mott scattering is one of the most important methods because of its high efficiency and stable operating character (Gay & Dunning, 1992; Dunning, 1994). In this method, transversely polarized electrons are scattered by a target of high atomic number, which results in a left–right scattering asymmetry of the scattering intensities due to the spin–orbit interaction. The inverse square of the statistical error of the polarization measurement is proportional to

$$\varepsilon = (I/I_0)S^2,$$

where I is the total number of scattered electrons detected, I_0 is the number of incident electrons and S is the Sherman asymmetry function. ε is termed as the efficiency of a Mott polarimeter (Kessler, 1985).

Recently, the retarding-potential Mott polarimeter has become one of the most widely used electron spin polarimeters because of its small size, high efficiency, good stability and possibility for self-calibration. Burnett *et al.* (1994) have reported a retarding type of Mott polarimeter with an efficiency of about 1.6×10^{-4} and dimensions of only about 10 cm.

In a synchrotron radiation laboratory, it is hoped that the spectrometer can be moved from one beamline to another to utilize the light with different characteristics. However, the most commonly available SARPES spectrometers at the moment are based on conventional Mott polarimeters which are difficult to move because of their large size. Moreover, only a few SARPES spectrometers can be used to measure spectra away from normal emission easily and most SARPES measurements reported to date only investigated electronic structures along the special symmetry line ($\overline{\Gamma}$ point) of the bulk (surface) Brillouin zone.

In this paper we report a new portable SARPES spectrometer which can be easily moved and can be used to measure the spectra away from normal emission.

2. Design considerations

The SARPES measurement system can be divided into three parts: preparation chamber, analyser chamber and polarimeter chamber. A schematic view is shown in Fig. 1. An Omicron SHA 50 simulated hemispherical angle-resolving electron energy analyser is positioned in the analyser chamber and can easily be rotated around the sample. A retarding-potential Mott polarimeter (Qiao *et al.*, 1997) is attached to the analyser to measure the spin polarization of the photoelectrons.

So far, electron detectors of Mott polarimeters have usually been set so as to accept scattered electrons centred about a 120° scattering angle, where the absolute value of the Sherman function of gold atoms takes its maximum (Gay & Dunning, 1992). However, in practice, a solid-state target instead of an atomic target is used and we have to consider the effective Sherman function in which multiple and plural scattering are included. The measurements of Gellrich & Kessler (1991) show that the maximum of the effective Sherman function of gold film is not at a scattering angle of 120°. Furthermore, for a larger collection

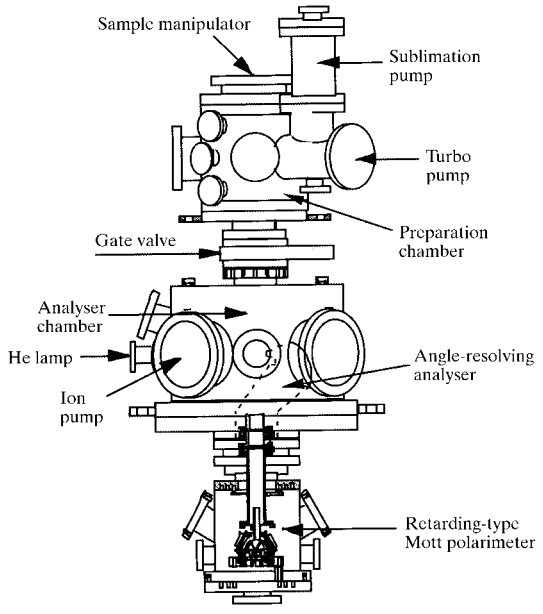

Figure 1
Schematic diagram of the spin- and angle-resolving photoelectron spectrometer.

angle of scattered electrons, although the scattering intensity is higher, the average Sherman function is smaller, so in pushing for a high efficiency it may be important to select a collection angle to compromise correctly between these two factors. Therefore, to design a Mott polarimeter with a high efficiency, we have to understand clearly the effective Sherman function and scattering intensity for different scattering angles. For a retarding-potential Mott polarimeter, the dependence of the above two functions on energy-loss windows is important. However, neither calculations nor accurate experimental investigations have been reported. We have carried out Monte Carlo calculations on the spin-dependent scattering process for 50 keV electrons incident on a gold target, and obtained the dependence of the effective Sherman function and the scattering intensity on the target thickness and inelastic energy-loss windows for scattering angles from 90 to 180° (Qiao & Kakizaki, 1997). The results show that the scattering intensity always takes its maximum at a scattering angle of about 120°, and, when the target is thicker than 700 Å or the inelastic energy-loss window is larger than 1200 eV (the typical values used practically), the effective Sherman function is almost constant over a wide range of scattering angles. Therefore, the electron detectors should be set near a scattering angle of 120°, not because of the maximum of the asymmetry function but because of the maximum of the scattering intensity at this scattering angle. The larger the collection angle for scattered electrons, the higher the efficiency of a Mott polarimeter.

A four-element lens system is used to transfer, accelerate and focus the electron beam from the analyser to the polarimeter target. When designing a lens system, the most important consideration is to choose the types and sizes of the elements to optimize the quality of the final image according to some criteria. In order to select the best structure, it is often possible to construct a suitable dimensionless figure of merit for a certain problem (Harting & Read, 1976). We divide our lens system into two parts. One part consists of the first three elements whose main purpose is to transfer the electron beam, and its magnification is set to be near unity. The other part, the final two elements, is used to focus the beam, and its magnification is set to be near zero. The geometrical and electrical parameters of the lens system were determined after referring to the data tables of the figure of merit for different lenses listed by Harting & Read (1976). The ray-tracing calculation result shows that, for the incident electron beam from the analyser with a radius of 2 mm and an opening angle of 12°, the radius of the image on the target is less than 0.3 mm and all of the electrons can reach the target without loss.

The most difficult and crucial part in designing a retarding-potential Mott polarimeter with a high efficiency is the retarding optics for the scattered electrons. The width of the energy-loss window is usually set to about 1000 eV and we intend to collect the scattered electrons with a large collection angle. Hence, special care should be taken to design the geometry and the applied voltages of the electrodes of the retarding optics to obtain both very small spherical and chromatic aberrations. Using the *CPO* three-dimensional *Charged Particle Optics Program* developed by R. B. Consultant Ltd, UK, a novel design was accomplished. The structure of the Mott polarimeter is shown in Fig. 2. The aperture of the outer sphere tends to focus the electron beam. The cylinder close to the outer sphere and the plane grid in the front of the multichannel plate (MCP) are used to direct the electrons to the MCP with an almost perpendicular direction with respect to the MCP plane, which results in an increase in the collection ability for the electrons with low kinetic energies, *i.e.* large energy losses. The calculated traces of the scattered electrons in the retarding optics are shown in Fig. 3. We can see that only the electrons with a 1500 eV energy loss and a 25° divergence fail to reach the MCP, so the collection solid angle achieved is about 0.59 sr, which is the largest collection angle for a retarding-potential Mott polarimeter reported so far.

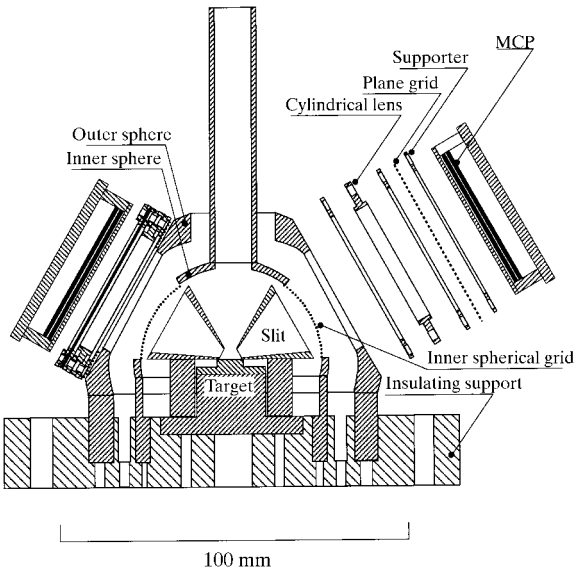

Figure 2
Structure of the retarding-potential Mott polarimeter.

3. Performance of the new SARPES spectrometer

To calibrate the effective Sherman function of our polarimeter, we used the polarized secondary electrons from an Ni(110) surface irradiated by an unpolarized electron beam, which have been studied by conventional Mott spin polarimeters calibrated

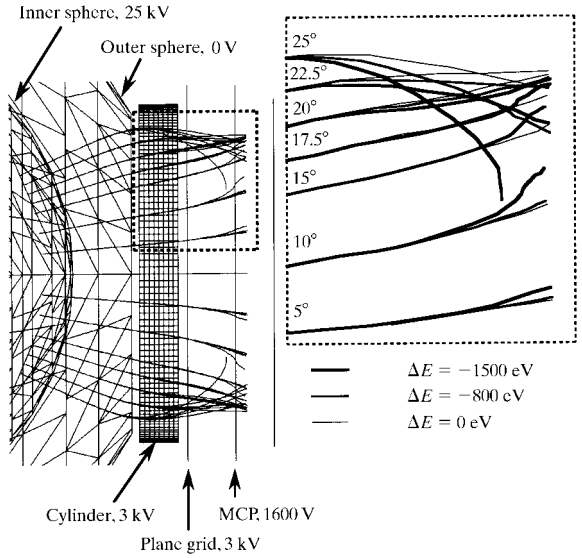

Figure 3
The trace of electrons in the retarding optics. The energy losses of electrons are set to be 1500, 800, 500 and 0 eV and the divergence angles are set to be 0, 5, 10, 15, 17.5, 20, 22.5 and 25°.

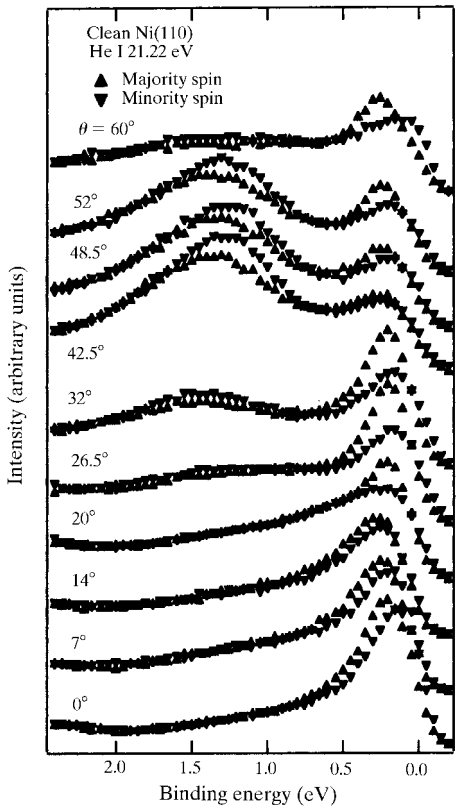

Figure 4
The spin- and angle-resolved photoelectron spectra of a clean Ni(110) surface measured along the $\overline{\Gamma S}$ line of its surface Brillouin zone excited by unpolarized He I radiation. The error bars in all the data points are smaller than the symbols. θ is the emission angle between the exit direction of the photoelectron and the normal of the Ni(110) sample.

by target thickness extrapolations (Hopster *et al.*, 1982; Landolt, 1985). The scattering intensity is measured by a method similar to that of Dunning *et al.* (1987), *i.e.* to compare the scattered electron count rate with the current entering the Faraday cup which is composed of the final lens element, inner sphere and target mount. We set the voltage of the Faraday cup to 600 V and the voltages of other lens elements to that determined by iteration using the *CPO* three-dimensional optics program to obtain the best focus on the gold target to ensure that all electrons can reach the Faraday cup. From the measured scattering intensity and effective Sherman function, the maximum efficiency of our polarimeter with a gold target is found to be $(1.9 \pm 0.2) \times 10^{-4}$ for a 25 kV operating voltage with an 800 eV energy-loss window. The corresponding scattering intensity and effective Sherman function are $(9.7 \pm 0.2) \times 10^{-3}$ and 0.14 ± 0.01, respectively. The efficiency of our polarimeter with a gold target is slightly larger than 1.6×10^{-4}, the highest efficiency of a retarding-potential Mott polarimeter, until now, reported by Burnett *et al.* (1994) using a thorium target. Dunning (1994) has stated that by replacing a gold target with a thorium target, the effective Sherman function and the scattering intensity increases by 10–20% and 15%, respectively. Hence, the efficiency of our polarimeter will increase to 2.9×10^{-4} by using a thorium target.

SARPES measurements (Raue *et al.*, 1983; Kakizaki *et al.*, 1997) have been used to study the spin-dependent electronic structure of nickel. However, most of the spin-resolved photoelectron measurements reported are performed only at normal emission. We measured the SARPES spectra of clean Ni(110), Ni(110)-$p(2\times1)$O and Ni(110)-$c(2\times2)$S along the $\overline{\Gamma S}$ line of the Ni(110) surface Brillouin zone for the first time. The spectra of clean Ni(110) are shown in Fig. 4. The structure at 1.3 eV binding energy emerges near the $\overline{S}$ point, corresponding to an emission angle of about 50°, and shows a large negative spin polarization.

We would like to express our thanks to Dr J.-G. Chung and Mr M. Sawada for their support of this work.

References

Burnett, G. C., Monroe, T. J. & Dunning, F. B. (1994). *Rev. Sci. Instrum.* **65**, 1893–1896.
Dunning, F. B. (1994). *Nucl. Instrum. Methods*, A**347**, 152–160.
Dunning, F. B., Gray, L. G., Ratliff, J. M., Tang, F. C., Zhang, X. & Walters, G. K. (1987). *Rev. Sci. Instrum.* **58**, 1706–1708.
Feder, R. (1985). Editor. *Polarized Electrons in Surface Physics.* Singapore: World Scientific.
Gay, T. J. & Dunning, F. B. (1992). *Rev. Sci. Instrum.* **63**, 1635–1651.
Gellrich, A. & Kessler, J. (1991). *Phys. Rev. A*, **43**, 204–216.
Harting, E. & Read, F. H. (1976). *Electrostatic Lenses.* Amsterdam: Elsevier Science.
Hopster, H., Raue, R., Kisker, E., Güntherodt, G. & Campagna, M. (1982). *Phys. Rev. Lett.* **50**, 70–73.
Kakizaki, A., Ono, K., Tanaka, K., Shimada, K. & Sendohda, T. (1997). *Phys. Rev. B*, **55**, 6678–6681.
Kessler, J. (1985). *Polarized Electrons*, 2nd ed. Berlin: Springer.
Landolt, M. (1985). *Polarized Electrons in Surface Physics*, edited by R. Feder, ch. 9. Singapore: World Scientific.
Qiao, S. & Kakizaki, A. (1997). *Rev. Sci. Instrum.* **68**, 4017–4021.
Qiao, S., Kimura, A., Harasawa, A., Sawada, M., Chung, J.-G. & Kakizaki, A. (1997). *Rev. Sci. Instrum.* **68**, 4390–4395.
Raue, R., Hopster, H. & Clauberg, R. (1983). *Phys. Rev. Lett.* **50**, 1623–1626.